Int J Clin Exp Med 2020;13(2):549-557
www.ijcem.com /ISSN:1940-5901/IJCEM0103835

Original Article

MiR-140-5p suppresses the adipogenic differentiation of mesenchymal stem cells in rats with steroid-induced osteonecrosis of the femoral head

Shengjun Lu[1], Baiwen Qi[1], Quanming Liao[2], Aixi Yu[1]

[1]*Department of Orthopedics, Zhongnan Hospital of Wuhan University, Wuhan, Hubei, China;* [2]*Department of Orthopaedics, Jingzhou Centre Hospital, Jingzhou, Hubei, China*

Received October 22, 2019; Accepted November 21, 2019; Epub February 15, 2020; Published February 28, 2020

Abstract: Objective: To explore the effects of miRNA-140-5p on all-trans retinoic acid (ATRA)-induced inhibition of the adipogenic differentiation of mesenchymal stem cells (MSCs) in rats with steroid-induced osteonecrosis of the femoral head (SONFH). Methods: A SONFH rat model was constructed. MSCs were isolated and induced to undergo adipogenic differentiation by inhibiting miRNA-140-5p expression and/or ATRA treatment. Samples were divided into six groups according to the following interventions: control group (N); miR-NC (A), negative control of miR-140-5p-inhibitor); siRNA-miR-140-5p (B); ATRA (C); ATRA + miR-NC (D); and ATRA + siRNA-miR-140-5p (E). After transfection with miR-NC and siRNA-miR-140-5p in MSCs, all trans-retinoic acid was added at a dose of 1 μmol/L. miRNA-140-5p expression levels were detected using qRT-PCR, and fat content was quantitatively determined using oil red O staining. Retinoic acid receptor (RARα, RARβ, and RARγ) and lipogenic differentiation marker (C/EBPβ and PPAR-γ protein) expression levels were detected using enzyme-linked immunosorbent assay. Osteopontin and osteocalcin expression levels were detected using Western blot. Results: Oil red O staining demonstrated that miR-140-5p knockdown or ATRA treatment significantly reduced cell fat content ($P < 0.05$). ATRA treatment inhibited RARα and RARγ expressions and promoted RARβ expression, which was also promoted by miR-140-5p knockdown ($P < 0.05$). Compared with the use of all-trans retinoic acid alone, simultaneous inhibition of miR-140-5p expression promoted the expression of retinoic acid receptor RARβ ($P < 0.05$), enhanced the induction of osteogenic differentiation of bone marrow mesenchymal stem cells ($P < 0.05$) and further inhibited adipogenic differentiation ($P < 0.05$). Thus, miR-140-5p expression inhibition or ATRA treatment can promote osteogenic differentiation and inhibit adipogenic differentiation of MSCs ($P < 0.05$). Conclusions: miR-140-5p knockdown combined with ATRA leads to an increase in RARβ expression and a stronger inhibition of adipogenic differentiation of MSCs than ATRA treatment alone.

Keywords: miRNA-140-5p, ATRA, SONFH, MSC, adipogenic differentiation

Introduction

Steroid necrosis of the femoral head (SONFH), also known as avascular necrosis or aseptic necrosis of the femoral head, is a bone metabolic disease that is caused by extensive treatment with glucocorticoids. It manifests as ischemic necrosis in the local bone trabecula and bone marrow, with collapse and fracture of the femoral head, and impaired hip function, which are induced by the turbulent intra-osseous environmental and depleted local blood supply [1, 2].

Currently, the primary treatment for clinical immunity diseases, along with other diseases, is hormone therapy, which is known to increase the incidence of SONFH [3, 4]. Reportedly, the proportion of femoral head necrosis caused by hormone therapy exceeds that caused by trauma and is the primary cause of non-traumatic femoral head necrosis [5]. SONFH is characterized by rapid onset and a high disability rate, which severely impair the quality of life of patients [6].

The pathogenesis of SONFH is not clearly understood. One of its known causes is the stimulation of bone marrow stromal stem cells (BMSSCs) by glucocorticoids to differentiate into fat cells. The differentiation results in a series of pathological changes such as fat

metabolism disorders and osteoporosis; causing femoral head necrosis [7, 8].

Therefore, regulating the adipogenic differentiation of BMSSCs is important for the treatment of SONFH. Recently, all-trans retinoic acid (ATRA) has been shown to efficiently inhibit the differentiation of MSCs into adipocytes. Liu et al. [9] reported that ATRA stimulates the osteogenic differentiation of preadipocytes induced by a bone morphogenetic protein-9, BMP/Smad, and Wnt/β-catenin signaling and inhibits adipogenic differentiation. The knockdown of β-catenin blocks the stimulation of BMP-9-induced alkaline phosphatase activity by ATRA and decreases the ability of ATRA to inhibit fat formation in MSCs via BMP-9 expression. Zhang et al. [10] reported that ATRA inhibited the adipogenic differentiation of MSCs through the RARγ-c-fos-PPARγ2 signaling pathway. However, the complete mechanism by which ATRA inhibits the adipogenic differentiation of MSCs remains unclear. In previous studies, the regulation of cell differentiation by ATRA was affected by single-stranded non-coding microRNA levels. Yang et al. [11] reported that inhibiting the expression of miRNA-146a can restore transforming growth factor-beta1 (TGF-β1) signaling by upregulating the expression of its target gene Smad4, which plays an important role in the differentiation of ATRA-induced acute promyelocytic leukemia cells. Therefore, the effects of ATRA are regulated by microRNAs. miR-140-5p is reported to be associated with adipogenic differentiation. Wang et al. [12] reported that miR-140-5p was significantly downregulated during adipogenic differentiation in human MSCs. Zhang et al. [13] also showed that miR-140-5p regulated adipocyte differentiation via C/EBP/miR-140-5p/TGF-βR receptor I (TGF-βR1) regulatory feedback. TGF-βR1 is known to be a direct target of miR-140-5p [13]. The knockout of miR-140-5p increased TGF-βR1 expression and inhibited the adipocyte differentiation of preadipocytes, thus promoting their osteogenic differentiation. How-ever, it is still unclear whether miR-140-5p has an effect on ATRA-induced inhibition of the adipogenic differentiation of MSCs.

In this study, a rat model of SONFH was established to explore the effects of miRNA-140-5p on ATRA-induced inhibition of the adipogenic differentiation of MSCs.

Materials and methods

Research subjects

Six healthy, male Sprague-Dawley rats were purchased from the Beijing Weitonglihua Experimental Animal Technology Co., Ltd [strain code, 101; production license number, SCXK (Beijing) 2012-0001]. They were fed the common nutritive feed (Beijing Zhecheng technology co., LTD.), and drinking water was acidified to a pH of 2.5-3 after sterilization by autoclave. The mean age of the rats was 57.4 ± 1.8 days, and their average body weight was 312 ± 9.7 g. The feed temperature was maintained at 18°C-22°C, and the relative humidity of the housing was 40%-70%. All rats were separately housed in the terrarium, and litter was cleaned every morning and evening. The ambient noise was maintained at ≤ 80 dB; the ammonia concentration was maintained at ≤ 20 ppm, and the air was ventilated 8-10 times per hour. Their housing was cleaned and disinfected, and replaced once or twice a week. The noise did not exceed 55 dB, and the ammonia concentration did not exceed 13 ppm. Moreover, fluorescent lamps were used for lighting at a 12-h light/dark cycle.

Establishing SONFH rat model

The rats were injected with endotoxin in the tail vein on the first day at a dose of 10 μg/kg. After 24 h, prednisolone acetate was subcutaneously injected at a dose of 21 mg/kg, and 80,000 U of penicillin was administered to prevent infection. The injection was administered once every 24 h for three consecutive days. X-ray visualization was used to evaluate the rat models.

MSC extraction and culture

Forty-eight hours after successful modeling, rats were subjected to ether inhalation for 3 min and were then sacrificed by intraperitoneally injecting pentobarbital (50 mg/kg). The rat tibia and femur were collected and washed under aseptic conditions before opening the epiphysis region. The bone marrow was washed out with cell growth media. After centrifugation at 1,000 rpm for 10 min, the supernatant was collected and resuspended to form a single-cell suspension, which was inoculated into complete medium. The inoculation density was 5 ×

Table 1. Primer sequence

	Upstream primer	Downstream primer
U6	CTCGCTTCGGCACA	AACGCTTCACGAATTTGCGT
miR-140-5p	GAGTGTCAGTGGTTTTACCCT	GCAGGGTCCGAGGTATTC

10^4/mL, and the cells were cultured in an incubator at 5% CO_2 and 37°C to obtain third generation MSCs for subsequent use. Flow cytometry was used to identify bone marrow derived MSCs by detecting the markers CD29, CD44, CD45, CD90, CD34, and CD11b on the surface of MSCs.

Intervention methods

Briefly, siRNA-miR-140-5p and miR blank vector (miR-NC) were designed and synthesized by Thermo Fisher Scientific. MSCs were trypsinized for 24 h before transfection, and the expression vector was transfected according to the manufacturer's instructions when the cells were fused to approximately 80% (20 pmpl of the expression vector and 1 μl of Lipofectamine 2000). The medium was cultured for 48 h in a 5% CO_2 incubator at 37°C, and the medium was changed every 6 h. Untreated MSCs were used as negative controls (control group, N).

After transfection, media was replaced with adipogenic differentiation medium (Jiangsu Punuosheng Biotechnology Co., Ltd., lot No. C-28011) for inducing adipogenic differentiation, and ATRA, miR-NC, or siRNA-miR-140-5p were simultaneously added. Samples were divided into six groups: control group, miR-NC, siRNA-miR-140-5p, ATRA alone, ATRA + miR-NC, and ATRA + siRNA-miR-140-5p. The formation of fat droplets indicated the end of fat induction. The dose of ATRA (Shanghai Beinuo Biotechnology Co., Ltd.; lot number, R2625-100MG) was 1 μmol/L [14]. After transfection, the medium was changed to adipogenic differentiation medium for adipogenic differentiation, and all-trans retinoic acid was added for intervention.

qRT-PCR

MSC suspension was adjusted to 1×10^7 cells/mL, and TRIzol™ reagent was added at a ratio of 3:1 for total RNA extraction. After extraction, RNA integrity was analyzed using 1.5% agarose gel electrophoresis. The purity of extracted RNA was assessed with a micronucleic acid analyzer, and A260/A280 ratios were considered satisfactory if they were between 1.8 and 2.1. After RNA extraction, reverse transcription reactions were performed; first strand cDNA was synthesized and then amplified using PCR. The PCR amplification reaction included 2 μL of cDNA template, 1 μL of diluted cDNA, 5 μL of 2*SYBR Green mixture, 1 μL each of the upstream and downstream primers, and double distilled water added to 10 μL. This was followed by 40 cycles of pre-denaturation at 94°C for 30 s, denaturation at 94°C for 5 s, and annealing at 60°C for 30 s. Dissolution curve analysis was performed at the end of the experiment. U6 was used as an internal reference. The results were analyzed using the $2^{-\Delta\Delta Ct}$ method. TRIzol™ Reagent was purchased from Chengdu Dongsheng Kechuang Technology Co., Ltd. (lot number, 15596026). The SYBR GREEN real-time fluorescent quantitative PCR kit was purchased from Nanjing Kebai Biotechnology Co., Ltd., (lot number, 4310251). The primer sequence was designed and synthesized by Herzen Biotechnology Co., Ltd. (Shanghai) (**Table 1**).

Enzyme-linked immunosorbent assay (ELISA)

ELISA was used to detect MSC surface expression of retinoic acid receptors (RARα, RARβ, and RARγ), C/EBPβ, and PPAR-γ as adipogenic differentiation markers on bone marrow as per the manufacturer's protocol. RARα, RARβ, and RARγ detection kits were purchased from Shanghai Jingkang Biological Engineering Co., Ltd. (lot numbers, JK-(a)-E03755, JK-(a)-E03754, and JK-(a)-E03753, respectively). C/EBPβ and PPAR-γ detection kits were purchased from Changsha Dalfeng Biotechnology Co., Ltd. (lot numbers, EBRK1320H1/H2 and BRK_0368R1, respectively).

Western blot analysis

Cell proteins were extracted suing the repeated freeze-thaw method and separated using polyacrylamide gel electrophoresis. Initially, voltage was set to 90 V and was then increased to 120 V to move the sample to an appropriate position on the separation gel. After electrophoresis, the film was subjected to 100 V for 100 min, and the gel was sealed for 60 min at 37°C. The transfer membrane was then blocked in

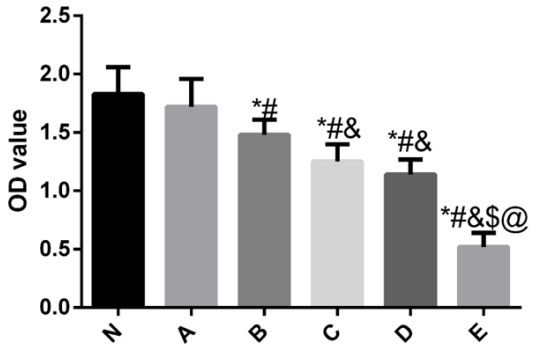

Figure 1. Quantitative determination of fat content. * indicates P < 0.05 compared with the control group; # indicates P < 0.05 compared with the A group; & indicates P < 0.05 compared with the B group; $ indicates P < 0.05 compared with the C group; @ indicates P < 0.05 compared with the D group; N: control group; A: miR-NC group; B: siRNA-miR-140-5p group; C: All-trans retinoic acid + control group; D: All-trans retinoic acid + miR-NC group; E: All-trans retinoic acid + siRNA-miR-140-5p group.

5% skim milk and incubated with primary antibody (1:1000) [anti-osteopontin (OPN) antibody from R&D Systems Inc, Minneapolis, USA; lot number, MAB14331; anti-osteocalcin (OC) antibody from Thermo Fisher Scientific, Massachusetts, USA; lot number, MA1-20788] at 4°C for 16 h. Cells were then washed three times with PBS for 5 min and incubated with Goat anti-mouse IgG secondary antibody (1:1000; Santa Cruz Biotechnology, CA, USA) for 1 h at room temperature using β-actin as an internal control. Blots were visualized using ECL luminescent reagent, and the images were statistically analyzed using Quantity One software. The relative expression levels of protein were equal to the band gray value/internal parameter gray value. The western blot test kit used was purchased from Shanghai Youyu Biotechnology Co., Ltd. (lot number, JC-445).

Oil red O staining

After 2 weeks of culture in adipogenic differentiation medium, the cells were washed with PBS, fixed with 4% neutral formaldehyde at RT for 30 min, and washed twice with PBS for 5 min to remove residual formaldehyde. Then, 3 mL of oil red O dye solution (0.5 g, 50% ethanol 100 mL) was added, and cells were incubated at RT for 30 min. This was followed by washing three times with PBS to remove excess oil red O. Subsequently, 200 μL of isopropanol was added and allowed to stand at RT for 5 min to dissolve the stain in the fat droplets. Fat content was then quantitatively determined by measuring the absorbance at 570 nm using a CLARIO star full-featured multi-function microplate reader (Boqi Technology Co., Ltd., Hong Kong).

Statistical methods

The statistical processing of data was performed using SPSS 19.0 (Asia Analytics, formerly SPSS China). Count data were expressed as means ± standard deviation (mean ± SD). One-way ANOVA was used for comparison among groups; the LSD test was used as the post hoc test. Moreover, the Pearson's correlation coefficient was used to measure the correlation between miRNA-140-5p and PARβ protein. P < 0.05 indicated a statistically significant difference.

Results

Quantitative determination of fat content

Significant differences were noted among the six groups with regard to fat content in the cells (all P < 0.001). Fat content in the B, C, D, and E groups were significantly lower than those in the control (N) and A groups (all P < 0.05). Fat content in the C, D, and E groups was significantly lower than that in the B group (all P < 0.05) and that in the E group was significantly lower than that in the C and D groups (all P < 0.05) (**Figure 1**).

RARα, RARβ, and RARγ expression level

Significant differences were noted among the six groups regarding RARα, RARβ, and RARγ expression levels (all P < 0.001). RARα and RARγ expression levels in the C, D, and E groups were significantly lower than those in the control (N), A, and B groups (all P < 0.05). RARβ expression level in the B, C, D, and E groups was significantly higher than that in the N and A groups (all P < 0.05); that in the C, D, and E group was significantly higher than that in the B group (all P < 0.05); and that in the E group was significantly higher than that in the C and D groups (all P < 0.05) (**Table 2**).

miR-140-5p expression levels

miR-140-5p expression levels among the six groups were significantly different (all P <

Table 2. RARα, RARβ, and RARγ expression levels (μmol/L)

	N	A	B	C	D	E	F	P
RARα	0.042 ± 0.003	0.041 ± 0.003	0.042 ± 0.002	0.035 ± 0.002$^{*,\#,\&}$	0.034 ± 0.003$^{*,\#,\&}$	0.035 ± 0.003$^{*,\#,\&}$	12.246	<0.001
RARβ	0.031 ± 0.002	0.032 ± 0.002	0.042 ± 0.003$^{*,\#}$	0.052 ± 0.003$^{*,\#,\&}$	0.053 ± 0.002$^{*,\#,\&}$	0.063 ± 0.003$^{*,\#,\&,\$,@}$	149.446	<0.001
RARγ	0.069 ± 0.004	0.067 ± 0.004	0.068 ± 0.005	0.024 ± 0.002$^{*,*,\#,\&}$	0.022 ± 0.003$^{*,\#,\&}$	0.023 ± 0.002$^{*,\#,\&}$	44.620	<0.001

Note: * indicates P < 0.05 compared with the control group; # indicates P < 0.05 compared with the A group; & indicates P < 0.05 compared with the B group; $ indicates P < 0.05 compared with the C group; @ indicates P < 0.05 compared with the D group; A: miR-NC group; B: siRNA-miR-140-5p group; C: all-trans retinoic acid (ATRA) + GC; D: ATRA + miR-NC; and E: ATRA + siRNA-miR-140-5p.

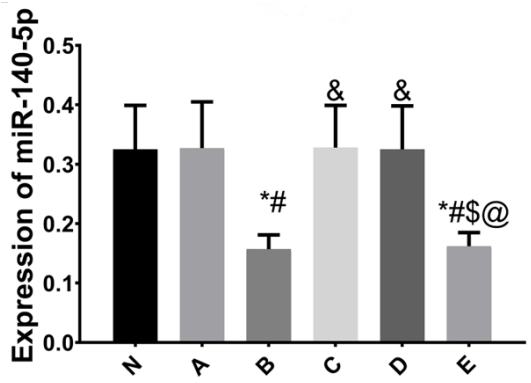

Figure 2. miR-140-5p expression levels. * indicates P < 0.05 compared with the control group; # indicates P < 0.05 compared with the A group; & indicates P < 0.05 compared with the B group; $ indicates P < 0.05 compared with the C group; @ indicates P < 0.05 compared with the D group; N: control group; A: miR-NC group; B: siRNA-miR-140-5p group; C: All-trans retinoic acid + control group; D: All-trans retinoic acid + miR-NC group; E: All-trans retinoic acid + siRNA-miR-140-5p group.

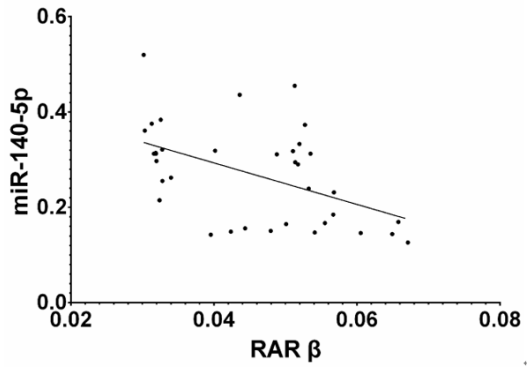

Figure 3. Correlation between miRNA-140-5p and PARβ expressions. r = -0.493, P = 0.002.

0.001) with those in the B and E groups being significantly lower than those in the control (N), A, C, and D groups (P < 0.05) (**Figure 2**).

Correlation between miRNA-140-5p and PAR β expressions

According to the Pearson's correlation coefficient, miRNA-140-5p and PARβ expressions were negatively correlated (P < 0.05) (**Figure 3**).

C/EBPβ and PPAR-γ expression levels

C/EBPβ and PPAR-γ expression levels significantly differed among the six groups (P < 0.001). These levels in the B, C, D, and E groups were lower than those in the control (N) and A groups (P < 0.05). These levels in the C, D, and E groups were lower than those in the B group (P < 0.05) and those in the E group were lower than those in the C and D groups (P < 0.05) (**Table 3**).

OPN and OC expression levels

Significant differences were noted in OPN and OC expression levels among the six groups (P < 0.001). These levels in the B, C, D, and E groups were higher than those in the control (N) and A groups (P < 0.05), while those in the C, D and E groups were higher than those in the B group (P < 0.05). This value in the E group was higher than that in the C and D groups (P < 0.05) (**Table 4**; **Figure 4**).

Discussion

SONFH is primarily caused by excessive hormone therapy, which causes an imbalance in the adipogenic differentiation and osteogenic differentiation of BMSSCs. This can lead to a series of pathological changes, including bone necrosis, which is caused by the excessive accumulation of lipids. Recently, the incidence of SONFH in clinical settings has increased [15, 16]. ATRA is a metabolite of vitamin A, and recent studies have found that ATRA has a significant effect in regulating lipid metabolism [17, 18]. Moreover, miR-140-5p has been reported to be involved in adipogenic differentiation [19, 20]. However, no studies have reported the effect of miR-140-5p on ATRA-

Table 3. C/EBPβ and PPAR-γ expression levels (μmol/L)

	Control	A	B	C	D	E	F	P
C/EBPβ	4.132 ± 0.811	4.034 ± 0.832	3.103 ± 0.712$^{*,\#}$	2.086 ± 0.543$^{*,\#,\&}$	2.104 ± 0.585$^{*,\#,\&}$	1.458 ± 0.327$^{*,\#,\&,\$,@}$	19.994	< 0.001
PPAR-γ	2.853 ± 0.303	2.651 ± 0.304	1.742 ± 0.259$^{*,\#}$	1.033 ± 0.217$^{*,\#,\&}$	1.042 ± 0.224$^{*,\#,\&}$	0.583 ± 0.116$^{*,\#,\&,\$,@}$	86.444	< 0.001

Note: * indicates P < 0.05 compared with the control group; # indicates P < 0.05 compared with the A group; & indicates P < 0.05 compared with the B group; $ indicates P < 0.05 compared with the C group; @ indicates P < 0.05 compared with group D; A: miR-NC group; B: siRNA-miR-140-5p group; C: ATRA + GC; D: ATRA + miR-NC; and E: ATRA + siRNA-miR-140-5p.

Table 4. OPN and OC expression level

	Control	A	B	C	D	E	F	P
OPN	0.103 ± 0.012	0.108 ± 0.013	0.211 ± 0.015$^{*,\#}$	0.328 ± 0.021$^{*,\#,\&}$	0.332 ± 0.025$^{*,\#,\&}$	0.426 ± 0.028$^{*,\#,\&,\$,@}$	262.515	< 0.001
OC	0.085 ± 0.009	0.082 ± 0.011	0.147 ± 0.012$^{*,\#}$	0.285 ± 0.022$^{*,\#,\&}$	0.279 ± 0.021$^{*,\#,\&}$	0.353 ± 0.025$^{*,\#,\&,\$,@}$	253.188	< 0.001

Note: * indicates P < 0.05 compared with the control group; # indicates P < 0.05 compared with the A group; & indicates P < 0.05 compared with the B group; $ indicates P < 0.05 compared with the C group; @ indicates P < 0.05 compared with the D group; A: miR-NC group; B: siRNA-miR-140-5p group; C: ATRA + GC: D: ATRA + miR-NC; and E: ATRA + siRNA-miR-140-5p.

induced inhibition of the adipogenic differentiation of MSCs. The present study aimed to address this issue.

In this study, we established a SONFH rat model using prednisolone acetate. The effects of miR-140-5p expression inhibition and/or ATRA treatment on the adipogenic differentiation of MSCs were then observed. We demonstrated that miR-140-5p expression inhibition or ATRA treatment resulted in a significant decrease in fat content in cells compared with that in untreated cells. Simultaneously applying both the treatments had a greater effect than either intervention alone. Measuring the expression levels of the adipogenic differentiation markers C/EBPβ and PPAR-γ [21, 22] revealed that their expression levels were significantly inhibited after treatments. This suggests that the adipogenic differentiation of MSCs was inhibited. Inhibition was further increased with the simultaneous use of the two treatments. Measuring the expression levels of osteogenic differentiation markers OPN and OC [23, 24] showed that the osteogenic differentiation of MSCs was enhanced after the treatments. These results [25, 26] suggest that miR-140-5p increased ATRA-induced inhibition of the adipogenic differentiation of MSCs. To explore the underlying mechanism, retinoic acid receptor (RARα, RARβ, and RARγ) expression levels were further examined. The results showed that miR-140-5p expression inhibition reduced RARβ expression and that miRNA-140-5p expression was negatively correlated with PARβ expression (according to Pearson's correlation coefficient). This was similar to the effects of ATRA treatment observed in this study: RARβ expression increased and RARα and RARγ expressions decreased. This may be one of the mechanisms by which miR-140-5p enhances ATRA-induced inhibition of the adipogenic differentiation of MSCs. Promoting the expression levels of retinoic acid receptor RARβ can enhance the effect of ATRA treatment on the inhibition of the adipogenic differentiation of MSCs. However, no studies have reported functional interaction between miR-140-5p and ATRA. Therefore, more experiments are warranted to corroborate the results of this study, and we hope that additional scholars are drawn to participate in this research.

This study has some limitations. For example, there are differences between our SONFH rat model and human SONFH. One important difference is that the rats used in this study were not mechanically loaded, and mechanical weight-bearing is an important cause of SONFH [27]. In future studies, the model can be improved by including forced fatigue exercises, such as running. Considering the overall differences between humans and rats, further verification is required to determine the generalizability of our findings to humans.

In conclusion, miR-140-5p expression inhibition to an increase in the expression of the retinoic acid receptor RARβ; moreover, ATRA-induced adipogenic differentiation of MSCs was strongly inhibited in a SONFH rat model.

Disclosure of conflict of interest

None.

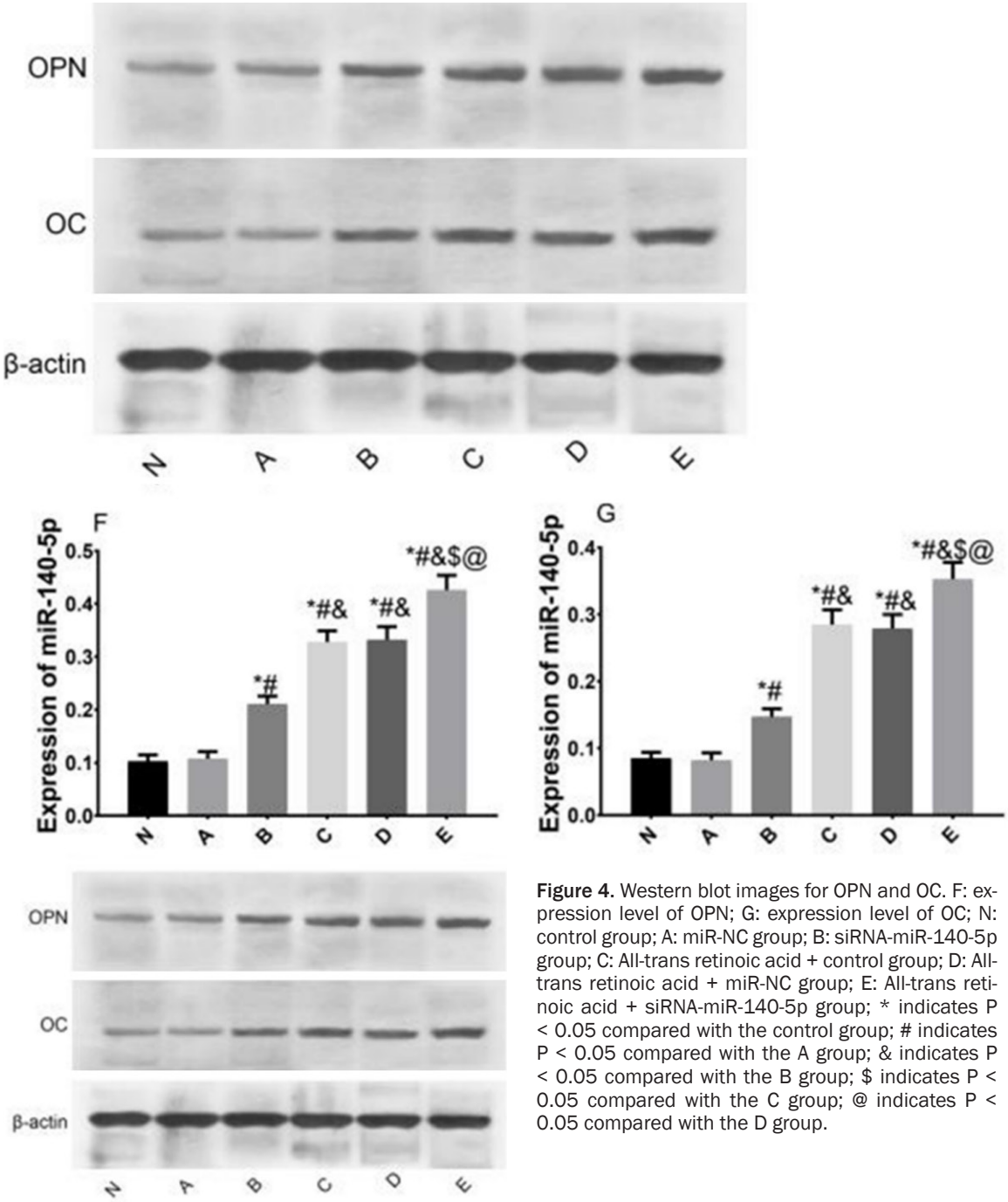

Figure 4. Western blot images for OPN and OC. F: expression level of OPN; G: expression level of OC; N: control group; A: miR-NC group; B: siRNA-miR-140-5p group; C: All-trans retinoic acid + control group; D: All-trans retinoic acid + miR-NC group; E: All-trans retinoic acid + siRNA-miR-140-5p group; * indicates $P < 0.05$ compared with the control group; # indicates $P < 0.05$ compared with the A group; & indicates $P < 0.05$ compared with the B group; $ indicates $P < 0.05$ compared with the C group; @ indicates $P < 0.05$ compared with the D group.

Address correspondence to: Aixi Yu, Department of Orthopedics, Zhongnan Hospital of Wuhan University, No. 169 Donghu Road, Wuchang District, Wuhan 434020, Hubei, China. Tel: +86-181071-67319; E-mail: ze4dh11@163.com

References

[1] Yang F, Luo P, Ding H, Zhang C and Zhu Z. Collagen type V a2 (COL5A2) is decreased in steroid-induced necrosis of the femoral head. Am J Transl Res 2018; 10: 2469-2479.

[2] Song Q, Ni J, Jiang H and Shi Z. Sildenafil improves blood perfusion in steroid-induced avascular necrosis of femoral head in rabbits via a protein kinase G-dependent mechanism. Acta Orthop Traumatol Turc 2017; 51: 398-403.

[3] Cui D, Zhao D and Huang S. Beneficial contribution of a safflower (Carthamus tinctorius L.)

polysaccharide on steroid-induced avascular necrosis of the femoral head in rats. Int J Biol Macromol 2019; 123: 581-586.
[4] Lin Z and Lin Y. Identification of potential crucial genes associated with steroid-induced necrosis of femoral head based on gene expression profile. Gene 2017; 627: 322-326.
[5] Ren X, Fan W, Shao Z, Chen K, Yu X and Liang Q. A metabolomic study on early detection of steroid-induced avascular necrosis of the femoral head. Oncotarget 2018; 9: 7984-7995.
[6] Jia YB, Jiang DM, Ren YZ, Liang ZH, Zhao ZQ and Wang YX. Inhibitory effects of vitamin E on osteocyte apoptosis and DNA oxidative damage in bone marrow hemopoietic cells at early stage of steroid-induced femoral head necrosis. Mol Med Rep 2017; 15: 1585-1592.
[7] Wei Q, Yang F, Chen X, He M, Chen Z, Zhang Q and He W. Microarchitecture features and pathology of necrotic region in patients with steroid-induced and alcohol-induced osteonecrosis of femoral head. Zhongguo Xiu Fu Chong Jian Wai Ke Za Zhi 2018; 32: 866-872.
[8] Yamamoto H, Saito M, Goto T, Ueshima K, Ishida M, Hayashi S, Ikoma K, Mazda O and Kubo T. Heme oxygenase-1 prevents glucocorticoid and hypoxia-induced apoptosis and necrosis of osteocyte-like cells. Med Mol Morphol 2019; 52: 173-180.
[9] Liu Y, Liu Y, Zhang R, Wang X, Huang F, Yan Z, Nie M, Huang J, Wang Y, Wang Y, Chen L, Yin L, He B and Deng Z. All-trans retinoic acid modulates bone morphogenic protein 9-induced osteogenesis and adipogenesis of preadipocytes through BMP/Smad and Wnt/beta-catenin signaling pathways. Int J Biochem Cell Biol 2014; 47: 47-56.
[10] Zhang S, Chen X, Hu Y, Wu J, Cao Q, Chen S and Gao Y. All-trans retinoic acid modulates Wnt3A-induced osteogenic differentiation of mesenchymal stem cells via activating the PI3K/AKT/GSK3beta signalling pathway. Mol Cell Endocrinol 2016; 422: 243-253.
[11] Yang S, Zhong H, Chen FY, Wang HR, Wang LM, Zhong JH and Huang HH. Change of miRNA-146a in all-trans retinoic acid-induced differentiation of NB4 cell lines and its effects. Tumor 2009; 29: 423-427.
[12] Wang T, Yan RQ, Cao J, Cao LL, Zhang XP, Li XN, Wu P, Zhou XO, Wu JF and Xu XY. Expression of miR-140-5p and prediction of its target gene in human mesenchymal stem cells during adipogenic differentiation. Nan Fang Yi Ke Da Xue Xue Bao 2016; 37: 199-203.
[13] Zhang X, Chang A, Li Y, Gao Y, Wang H, Ma Z, Li X and Wang B. miR-140-5p regulates adipocyte differentiation by targeting transforming growth factor-beta signaling. Sci Rep 2015; 5: 18118.
[14] Mercader J, Palou A and Bonet ML. Induction of uncoupling protein-1 in mouse embryonic fibroblast-derived adipocytes by retinoic acid. Obesity 2010; 18: 655-662.
[15] Xie Y, Hu JZ and Shi ZY. MiR-181d promotes steroid-induced osteonecrosis of the femoral head by targeting SMAD3 to inhibit osteogenic differentiation of hBMSCs. Eur Rev Med Pharmacol Sci 2018; 22: 4053-4062.
[16] Meng CY, Liu WL, Bai R and Zhao ZQ. Cell autophagy is involved in steroid-induced necrosis of the femoral head. 2017.
[17] Li Z, Jin C, Chen S, Zheng Y, Huang Y, Jia L, Ge W and Zhou Y. Long non-coding RNA MEG3 inhibits adipogenesis and promotes osteogenesis of human adipose-derived mesenchymal stem cells via miR-140-5p. Mol Cell Biochem 2017; 433: 51-60.
[18] Zhang M, Li DH, Li F, Sun JW, Jiang RR, Li ZJ, Han RL, Li GX, Liu XJ, Kang XT and Sun GR. Integrated analysis of MiRNA and genes associated with meat quality reveals that Gga-MiR-140-5p affects intramuscular fat deposition in chickens. Cell Physiol Biochem 2018; 46: 2421-2433.
[19] Sakakura M, Nishii K, Usui E, Monma F, Tsukada T and Shiku H. Bilateral osteonecrosis of the head of the femur during treatment with retinoic acid in a young patient with acute promyelocytic leukemia. Int J Hematol 2006; 83: 252-253.
[20] Stoecker K, Sass S, Theis FJ, Hauner H and Pfaffl MW. Inhibition of fat cell differentiation in 3T3-L1 pre-adipocytes by all-trans retinoic acid: Integrative analysis of transcriptomic and phenotypic data. Biomol Detect Quantif 2017; 11: 31-44.
[21] Luo X, Ryu KW, Kim DS, Nandu T, Medina CJ, Gupte R, Gibson BA, Soccio RE, Yu Y, Gupta RK and Kraus WL. PARP-1 controls the adipogenic transcriptional program by PARylating C/EBP-beta and modulating its transcriptional activity. Mol Cell 2017; 65: 260-271.
[22] Wang LF, Miao LJ, Wang XN, Huang CC, Qian YS, Huang X, Wang XL, Jin WZ, Ji GJ, Fu M, Deng KY and Xin HB. CD38 deficiency suppresses adipogenesis and lipogenesis in adipose tissues through activating Sirt1/PPARγ signaling pathway. J Cell Mol Med 2017; 22: 101-110.
[23] Filipowska J, Reilly GC and Osyczka AM. A single short session of media perfusion induces osteogenesis in hBMSCs cultured in porous scaffolds, dependent on cell differentiation stage. Biotechnol Bioeng 2016; 113: 1814-1824.
[24] Kaneto CM, Pereira Lima PS, Prata KL, Dos Santos JL, de Pina Neto JM, Panepucci RA, Noushmehr H, Covas DT, de Paula FJA and Sil-

va WA Jr. Gene expression profiling of bone marrow mesenchymal stem cells from Osteogenesis Imperfecta patients during osteoblast differentiation. Eur J Med Genet 2017; 60: 326-334.

[25] Hwang S, Park SK, Lee HY, Kim SW, Lee JS, Choi EK, You D, Kim CS and Suh N. miR-140-5p suppresses BMP2-mediated osteogenesis in undifferentiated human mesenchymal stem cells. FEBS Lett 2014; 588: 2957-2963.

[26] Bi W, Gu Z, Zheng Y, Zhang X, Guo J and Wu G. Heterodimeric BMP-2/7 antagonizes the inhibition of all-trans retinoic acid and promotes the osteoblastogenesis. PLoS One 2013; 8: e78198.

[27] Sugioka Y, Hotokebuchi T and Tsutsui H. Transtrochanteric anterior rotational osteotomy for idiopathic and steroid-induced necrosis of the femoral head. Indications and long-term results. Clin Orthop Relat Res 1992; 111-120.